Observation of spin-glass-like behavior in $SrRuO_3$ epitaxial thin films

R. Palai,[1] H. Huhtinen,[2] J. F. Scott,[3] and R. S. Katiyar[1]
[1]*Department of Physics and Institute for Functional Nanomaterials, University of Puerto Rico, San Juan, Puerto Rico 00931-23343, USA*
[2]*Department of Physics, University of Turku, Turku FIN-20014, Finland*
[3]*Department of Earth Science, University of Cambridge, Cambridge CB2 1PZ, United Kingdom*
(Received 13 November 2008; revised manuscript received 26 January 2009; published 12 March 2009)

We report on the observation of spin-glass-like behavior and strong magnetic anisotropy in extremely smooth (~1–3 Å roughness) epitaxial (110) and (010) $SrRuO_3$ thin films. The easy axis of magnetization is always perpendicular to the plane of the film (unidirectional) irrespective of crystallographic orientation. An attempt has been made to understand the nature and origin of spin-glass behavior, which fits well with Heisenberg model.

DOI: 10.1103/PhysRevB.79.104413 PACS number(s): 75.50.Lk, 75.60.Ej, 75.70.Ak, 77.80.−e

I. INTRODUCTION

Integration of functional materials (oxides of ferroelectrics and multiferroics) into silicon technology is of great technological and scientific interests. The current interest in functional oxides is largely based on engineered epitaxial thin films because of their superior properties compared to the bulk and polycrystalline thin films and their technological applications in dynamic random access memories, magnetic recording, spintronics, and sensors.[1–3] Most of these applications require bottom and top electrodes to exploit the electronic properties of the functional materials.

$SrRuO_3$ (SRO) has been found to be very useful for electrodes and junctions in microelectronic devices because of its good electrical and thermal conductivities, better surface stability, and high resistance to chemical corrosion, which could minimize interface electrochemical reactions, charge injection in oxide, and other detrimental processes,[4,5] thus improving retention, fatigue resistance, and imprint. It also has good work function to produce the required large Schottky barrier on most ferroelectric oxide capacitors.[6] Growth of an atomically flat epitaxial SRO film is required for a smooth and stable interface which is essential for the growth of subsequent layers, as high imperfections and roughness in the base layer can induce defects in the upper layers, which can irreversibly destroy the material properties. However, recent studies of epitaxial thin films[7–9] suggest that SRO may have novel magnetostructural properties in ultrathin-film form. By tuning film thickness and in-plain strain very different properties may emerge as compared with bulk. It has been found that thin films of SRO show uniaxial magnetic anisotropy[7,8] instead of biaxial anisotropy observed in bulk.[10,11]

The bulk SRO exhibits an orthorhombic crystal structure (a=5.570 Å, b=5.530 Å, and c=7.856 Å)[12] and several useful properties, such as extraordinary Hall effect,[4] strong magnetocrystalline anisotropy,[7] itinerant ferromagnetism,[13,14] and spin-glass behavior.[15] Spin-glass materials are currently frontier field of research and the most complex kind of condensed state of matter encountered so far in solid-state physics. Despite of the enormous importance of spin-glass models in neural networks,[16] our knowledge of the underlying mechanistic processes involved is extremely limited. Some of the typical features of spin glass are spin freezing (very slow time relaxation of magnetization), a cusp in the temperature dependence of magnetization, irreversible behavior of magnetization below the freezing temperature, remanence, and magnetic hysteresis.[17,18] Although spin-glass-like behavior has been reported in bulk SRO, to our knowledge, the behavior is not well understood and there was no such report in thin films. In this paper, we report on the observation, interpretation, and possible origin of spin-glass-like behavior in very smooth epitaxial (110) and (010) SRO thin films and observation of spontaneous alignment of domains in (010) thin films.

II. EXPERIMENTAL DETAILS

We investigated SRO thin films of 25 nm thick grown on (100) and (110) $SrTiO_3$ (STO) substrates of area (5 mm)^2 by pulsed laser deposition (PLD). The growth parameters were as follow: substrate temperature of 750 °C, oxygen partial pressure of 100 mTorr, and laser energy density of 2.0 J cm^{-2} at a pulse rate of 10 Hz. X-ray diffraction (XRD) was used to investigate the orientation and crystallinity of films. Microstructure and growth mechanism of the films were studied using atomic force microscopy (AFM). Magnetic measurement was carried out using a superconducting quantum interference device (SQUID) magnetometer. Before the magnetic measurement the silver paint was removed from the back of the substrate to eliminate spurious magnetic signal.

III. RESULTS AND DISCUSSION

The XRD patterns (Fig. 1) of 25-nm-thick SRO films on (100) and (110) STO (cubic with a=3.905 Å) substrates show [110] and [010] orientations, respectively. The insets in Fig. 1 depict the schematic of growth orientation of SRO films on (100) and (110) STO substrates. The out-of-plane lattice parameter of [110] and [010] oriented SRO films was found to be d_{110}=3.932 Å and d_{010}=5.543 Å, respectively, which is slightly larger than the corresponding bulk value of d_{110}=3.924 Å and d_{110}=5.530 Å. This clearly implies that films have out-of-the-plane tensile strain. The in-plane lattice strain between STO_{100} and SRO_{110} and STO_{110} and SRO_{010} was calculated and found to be 0.5% compressive and this

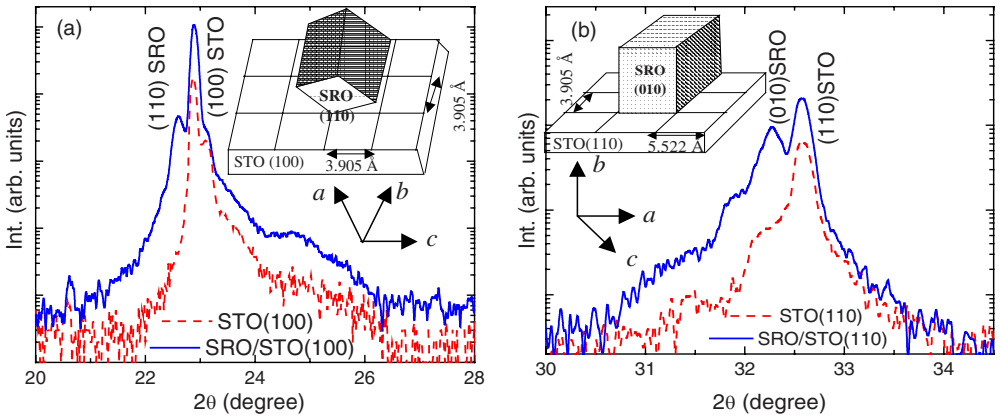

FIG. 1. (Color online) XRD patterns of SRO (a) (110) and (b) (010) films grown on (100) and (110) STO substrates, respectively. XRD pattern of STO is given for comparison. The insets depict the schematic of the growth orientations of SRO films on (100) and (110) STO substrates.

should result out-of-the-plane lattice parameter of 3.939 Å in [110] and 5.557 Å in [010] orientated films, which agrees with our observed values as strain gradually relaxes with increasing thickness.

Figure 2 shows the AFM images of SRO films on 2×2 μm^2 area. The surface morphology of both the films did not now show any 3D-like island or spiral-like growth, but rather two-dimensional (2D)-like layer-by-layer growth. However, a spontaneous alignment of the grains (magnetic domains) has been observed in [010] oriented film. The films were atomically smooth and the surface roughness (Z_{rms}) was found to be 1.3 and 2.1 Å in [110] and [010] oriented films on 2×2 μm^2 area, respectively, which is close to the AFM resolution. Functions, such as 2D Fourier transform or autocorrelation function can be used to quantify the aspect of the texture and lateral directionality of the surface topography. The asymmetry in the autocorrelation function quantifies the directionality of the features.[19] A scanning probe microscopy software[20] has been used for analyzing the autocorrelation function of the AFM images. Figures 2(c) and 2(d) are the 3D autocorrelation images of AFM surfaces (a) and (b), respectively. The symmetric nature of autocorrelation images shows excellent lateral directionality of the SRO films.

Figure 3 shows temperature dependence of hysteresis loops of (110) and (010) SRO films with applied field (B) perpendicular ($\perp$) and parallel ($\parallel$) to the plane of the film. The [110] oriented film showed maximum saturation magnetization (M_s) of about 19×10^4 A/m (190 emu/cc), while [010] oriented film showed 2 times higher magnetization than [110] oriented film. The possible explanation could be the presence of spontaneous alignment of the magnetic domains in [010] oriented film. The anomalies observed in the hysteresis loop at 5 K [less acute in the case of (010) film] between two regions of opposite field could be the Barkhausen jumps.[21] These jumps are generally caused by the irreversible motion of the domain walls between the two regions of opposite magnetizing forces. As evident from Fig. 3, there is only one easy axis of magnetization and it is always out of plane (perpendicular to the plane of the film) and perpendicular to the c axis, contrary to the earlier observation of easy axis along the c axis on SRO films on STO (100) substrates,[22] but in agreement with Refs. 7 and 23. The observed strong magnetic anisotropy could be the manifestation of spin-orbital coupling of ruthenium atoms or possibly due to the strong pinning of the domains perpendicular to the film. Materials with the easy axis of magnetization perpendicular to the surface have considerable importance in realizing the next generation perpendicular magnetic recording (PMR) system. Almost all the commercial recording systems available in the market use magnetic media with magnetization in the plane of film, known as longitudinal magnetic recording (LMR), and are limited by the superparamagnetic

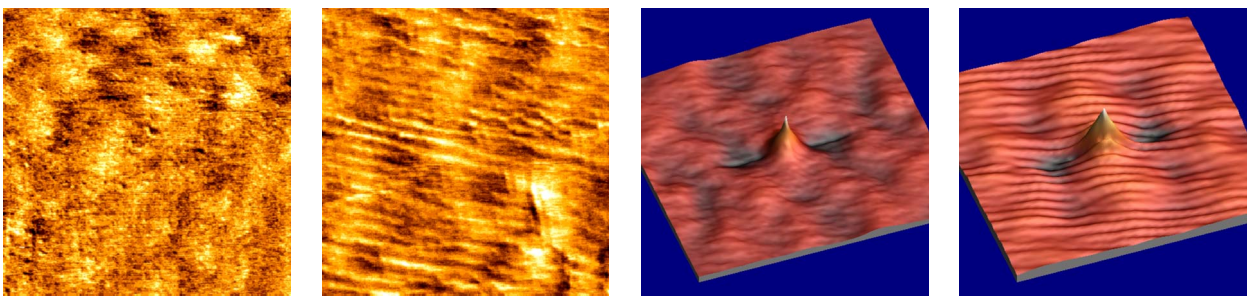

FIG. 2. (Color online) AFM images of SRO films on STO substrates. (a) [110] oriented SRO film on [100] STO substrate, (b) [010] oriented SRO film on [110] STO substrate, (c) and (d) are the three-dimensional (3D) autocorrelation images of the surfaces (a) and (b), respectively. The scan area was 2×2 μm^2.

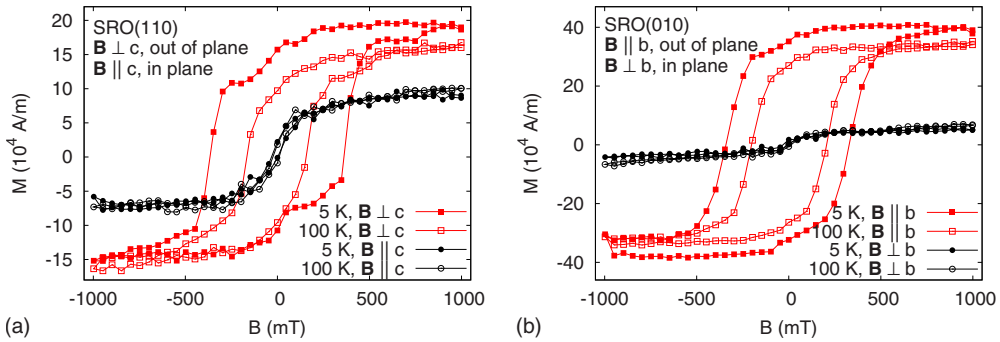

FIG. 3. (Color online) Temperature dependence of hysteresis (M-B) loops of SRO films on STO substrates at different orientations: (a) (110) SRO film and (b) (010) SRO film.

effect. The storage densities as high as 1 Tbit in.$^{-2}$ could be achieved with the PMR system,[24,25] where the superparamagnetic effect is less acute.

Temperature dependence of zero-field-cooled (ZFC) and field-cooled (FC) magnetizations of (110) and (010) SRO films recorded in different orientations with 100 mT are shown in Fig. 4. As can be seen, a unidirectional (always out of plane) anisotropy has been observed irrespective of the orientations. The magnetization also measured field in plane perpendicular to the c axis in SRO(110) films, but was found to be magnetically hard. The transition temperature was found to be 150 and 160 K for [110] and [010] orientated films, respectively. The out-of-plane FC spontaneous magnetization below T_c follows the scaling law $M=C(T_c-T)^{\beta}$ with critical exponent $\beta=0.369(\pm 0.006)$ and Curie constant $C=2.46(\pm 0.06)$ A/m for [110] oriented film indicating 3D Heisenberg-type ferromagnet (for which theory gives $\beta=0.367$);[26] whereas $\beta=0.313(\pm 0.007)$ and $C=7.45(\pm 0.25)$ A/m were obtained for [010] oriented film implying Ising (3D)-type ferromagnet (theoretical value of $\beta=0.326$).[26] However, there are some discrepancies in the literature. The exponent $\beta=0.43$ (Ref. 27) and 0.325 (Ref. 28) was obtained for [110] oriented 100-nm-thick films, while $\beta=0.5$ was obtained for single crystal[29] and interpreted as mean-field behavior (in our opinion this results from strain, which is always unscreened and hence long range). The difference in exponent value in our case could be related to different domain structures, orientation, or strain effect. We describe below a more detailed study of these behaviors.

The insets in Figs. 4(a) and 4(b) show plots of reduced magnetization $M(T)/M(0)$ vs $T^{3/2}$ in the low-temperature region, where $M(0)$ is the magnetization at 0 K, with the linear fit to the data. As evident, the magnetization behavior well describes the Bloch's law $M(T)/M(0)=1-AT^{3/2}$ (where A is the spin-wave parameter) implying the dominance of spin-wave excitation on magnetization as expected for a Heisenberg ferromagnet.[30] In itinerant ferromagnets, the low-temperature magnetization is further suppressed by a term T^2, which is due to Stoner excitations of magnetic electrons. The excellent fit to $T^{3/2}$ law is clearly observed in both the films even without the small T^2 correction, which implies the suppression of Stoner excitations. The fact that FC magnetization does not saturate at low temperature implies short-range spin ordering in SRO like spin glasses $La_{0.7-x}Nd_xPb_{0.3}MnO_3$ ($x=0.5$ and 0.7), which also follow Bloch's $T^{3/2}$ law.[31] The exchange interaction (J) between two neighboring Ru^{4+} ions was calculated using spin-wave parameter $A=(0.0587/S)(k_B/2JS)^{3/2}$, where S is the total spin of Ru^{4+} and k_B is the Boltzmann constant, and found to be $16.1k_B$ K and $21.37k_B$ K for [110] and [010] oriented films, respectively. The larger exchange energy for [010] oriented films is in agreement with the higher T_c observed. In comparison, J values of $14.41k_B$ K and $20.57k_B$ K have been reported for 100-nm-thick SRO films deposited by sputtering.[27]

Figures 5(a) and 5(c) show the temperature dependence of ZFC and FC magnetization at different fields applied out of plane (perpendicular to the plane of the film) for [110] and

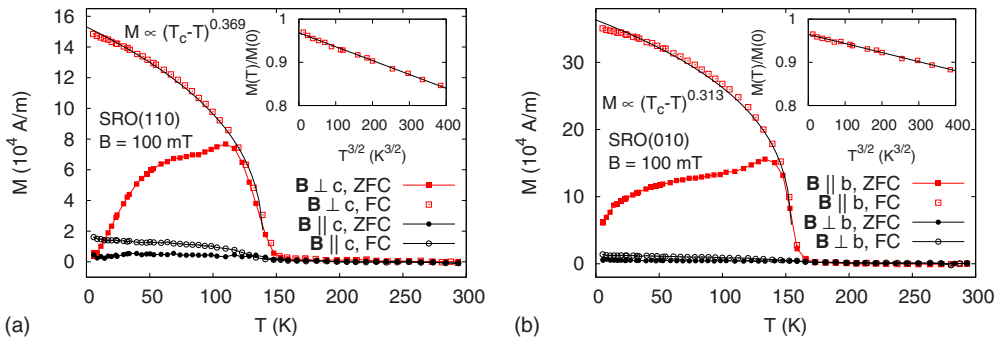

FIG. 4. (Color online) (a) ZFC and FC magnetizations of SRO films as a function of temperature at different orientations: (a) (110) SRO films and (b) (010) SRO film. The solid line on FC magnetizations is the curve fitted with $M \propto (T_c-T)^{\beta}$. The insets show the reduced magnetization $M(T)/M(0)$ vs $T^{3/2}$ in the low-temperature region. The straight lines are linear fit to the Bloch's law.

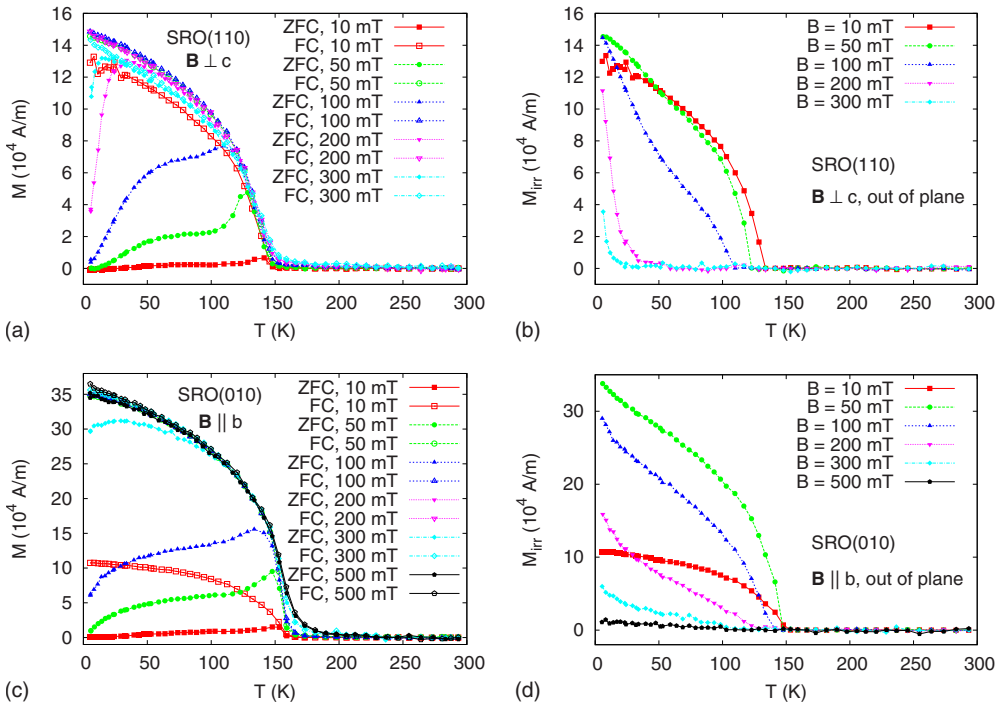

FIG. 5. (Color online) Temperature dependence of out-of-plane ZFC and FC magnetizations of (a) (110) and (c) (010) SRO films with their corresponding irreversibility magnetization M_{irr} vs T (b) (110) and (d) (010) SRO thin films.

[010] oriented films, respectively. A significant difference has been observed in ZFC and FC magnetizations. A closer observation of out-of-plane ZFC magnetization reveals three characteristic features: a critical temperature T_c, the onset of nonzero M, an irreversibility temperature T_g, where the ZFC and FC branches coalesce, and a pronounced cusp, which varies with field and gradually smoothens at higher fields. According to Edwards and Anderson[32] the latter one is because of the interaction of the spins dissolved in the matrix, as a result there is *no* mean ferro- or antiferromagnetism, but there will be a ground state with the spins aligned in definite directions. It is interesting to note that the out-of-plane FC magnetization with 10 mT for [010] oriented film is less compared to the [110] orientated film. This can be understood due to spontaneous alignment of the domains, the field of 10 mT is not adequate to align all the domains along the direction of the field.

The irreversible magnetization M_{irr} $(=M_{\mathrm{FC}}-M_{\mathrm{ZFC}})$ as a function of temperature for different fields is shown in Figs. 5(b) and 5(d) for [110] and [010] oriented films, respectively. The point at which M_{irr} becomes nonzero defines a spin-glass transition temperature T_g at the working field and the characteristic measuring time. The field dependence of $T_g(H)$, which increases with field, is the most important characteristic of spin glasses due to competing interactions because of frozen disorders and magnetic frustrations.[17,18,33] A spin-glass order parameter can be estimated from the field dependence of $T_g(H)$ that vanishes roughly linearly with temperature at freezing temperature (T_F).[17] Note that a spin glass cannot be described by a single order parameter, but rather requires many of them due to the existence of many phases.[18]

The exact nature of frozen disorder and frustration is not quite clear; however, possibly *spin canting* at low temperature might have produced *finite* spin clusters (composed of a set of noncollinear ferromagnetically or antiferromagnetically coupled spins), which are embedded in the *infinite* 3D ferromagnetic (FM) matrix.[18,34]

In order to understand the frozen state and freezing transition of SRO thin films, the behavior of magnetic field has been analyzed in the field-temperature plane. The existence of critical lines (Fig. 6) can be explained by mean-field theory (MFT) in the framework of replica-symmetry breaking.[17,18,33] The equations for the transition lines have been predicted by de Almeida and Thouless (called AT line) for Ising spin glass with infinite-range random interactions and by Gabay and Toulouse (called GT line) for the Heisenberg spin glass.[17,18,33,35]

The so-called AT line is usually defined as $H(T_g)$ and behaves near the freezing temperature as

$$\left(1-\frac{T_g(H)}{T_F}\right)^3=\frac{3}{4}h^2,\quad h=\frac{\mu H}{k_B T_F},\tag{1}$$

where T_F is the zero-field spin-glass freezing temperature. The GT line is defined as

$$1-\frac{T_g(H)}{T_F}=\frac{m^2+4m+2}{4(m+2)^2}h^2,\tag{2}$$

where m is the total number of the components (with $m-1$ transverse components) of the spin glass. At this line only the *transverse* components of the spins should be freezing in at the low temperature, while the freezing in of longitudinal components should occur at the crossover, which is similar to the AT line. The critical lines are defined by a dynamical instability and onset of broken ergodicity, as manifested by

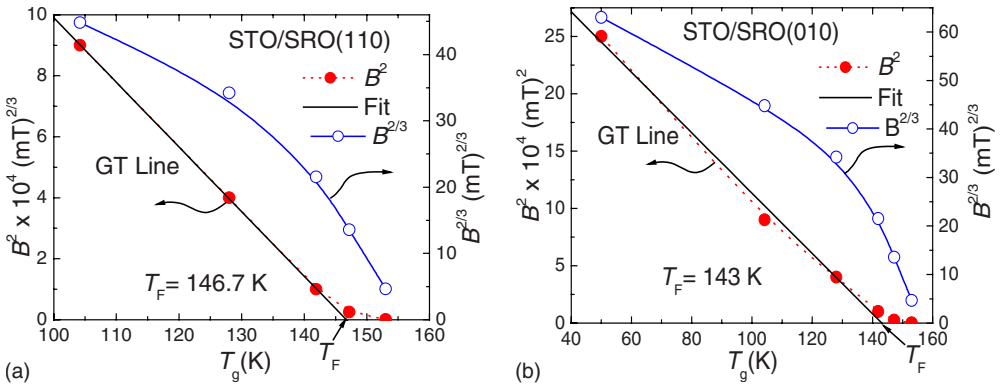

FIG. 6. (Color online) Field dependence of T_g raised to the square and 2/3 powers for (a) (110) and (b) (010) SRO films. The solid lines are the fitted to data points with Eq. (2).

irreversible effect due to the existence of a large number of degenerate thermodynamic states with the same microscopic properties but with different microscopic configurations.[17] The existence of critical line is one of the important fingerprints of spin glass.[17,18,33,35] In Fig. 6, the field dependence of T_g was raised to square and 2/3 powers in order to check the critical lines. Note that in this system it is difficult to clearly differentiate between Ising and Heisenberg spin glasses. However, as can be seen, the experimental data show a better fitting with Eq. (2) with GT line for $H > 100$ mT implying Heisenberg-type spin glass and the T_F was found to be $\approx 146.7(\pm 0.19)$ and $143(\pm 3)$ K for [110] and [010] oriented films, respectively. It is intriguing to note that the FC out-of-plane magnetization of [010] films at low field (100 mT) follows Ising-type ferromagnet (3D), but the overall behavior in *H-T* phase space agrees well with Heisenberg model. This can be understood as spin glasses have many metastable spin configurations and dynamics on many timescales and a complicated behavior is expected when spin glass coexists with FM orderings, called *magnetized spin glass*.[17]

In order to understand the characteristic excitation and relaxation time, we investigated both the isothermal remanent magnetization (σ_{IRM}) and thermoremanent magnetization (σ_{TRM}) of [110] and [010] oriented SRO films at 100 K (not shown) and 5 K (Fig. 7). σ_{IRM} was measured cooling the samples in zero field (ZFC) to the desired temperature to be studied; then a field of (100 mT) was applied for 10 min and switched off again, and the time relaxation was followed. To obtain σ_{TRM}, on the other hand, the sample was field cooled (100 mT) at some initial temperature [room temperature (RT)] above T_F and then the system was slowly cooled down in a constant field to the desired temperature (100 or 5 K), at which the field was switched off and the time relaxation was followed. As can be seen from Fig. 7, no exponential time decay, but rather a very *slow relaxation*, has been observed over macroscopic time scale indicating a large misfit at the domain walls causing extremely slow domain growth.[17] An extremely slow relaxation of magnetization with time below T_F is particularly an important and interesting salient feature of spin glasses.[17,18] This type of slow relation was reported in other FM spin-glass materials i.e., La_2CoMnO_6 (Ref. 36) and AuFe (Heisenberg-type FM)[37] alloy.[17,18]

A schematic of the phase diagram (Fig. 8) of SRO thin films was drawn from all measurements. We found that the spin-glass behavior is confined within ~1 T and ~150 K.

In $SrRuO_3$, Ru ions, known to be the only site of magnetic moment, are arranged in a strictly periodic order, which is unfavorable for a spin-glass state. SRO with tolerance factor (Goldschmidt) of 0.994 would not be expected to be distorted, but the polarized neutron-scattering experiments on single crystal showed the strong hybridization of Ru(4*d*)-O(2*p*) orbitals, which results in 10% of ordered magnetic moment associated with oxygen site;[38] approximately

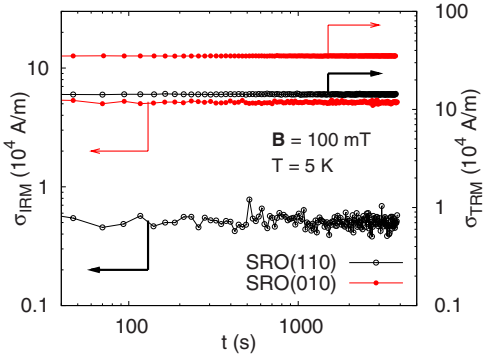

FIG. 7. (Color online) Time relaxation of isothermal remanent magnetization (σ_{IRM}) and thermoremanent magnetization (σ_{TRM}) of SRO thin films. The "open circle" represents that for [110] films, while "solid circle" that for [010] films.

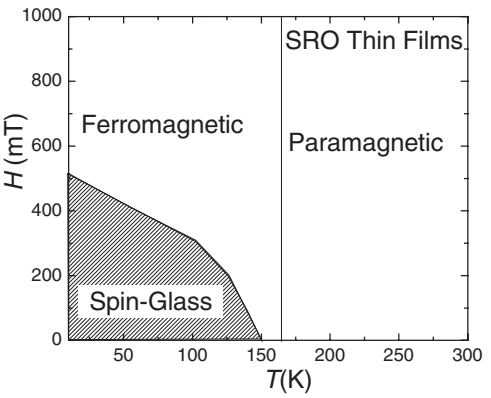

FIG. 8. Schematic of field-temperature (*H-T*) phase diagram of SRO thin films.

30% has been theoretically calculated.[39] We believe that this distribution of magnetic moments between the Ru sites and the O sites might have created the frustration and the randomness necessary for the spin glass. Recently, Zayak *et al.*[40] predicted that SRO also has weak *A*- and *C*-type antiferromagnetic (AFM) spin configurations along with most stable FM configuration. Our conjecture is that some AFM spin clusters (at Sr site) could have embedded into the FM matrix (at Ru site) causing the randomness necessary for the origin of spin-glass behavior. Epitaxial strain and small oxygen vacancy could trigger the change in the spin configurations and the shape of the octahedra in SRO thin films.

The spin-glass behavior can also be understood from the discrepancy between the calculated magnetic moment of $2.82\mu_B$ (for $S=1$ on the spin-only formula) and the measured magnetic moment from the saturation magnetization corresponds to the Curie constant of 2.46 A/m for [010] oriented film, leading to $\mu=3.19\mu_B$/f.u. The part of the moment which is being frozen out below T_F could be related to *magnetic domains*.

IV. CONCLUSION

In conclusion, spin-glass-like behavior was observed in high-quality [110] and [010] oriented SRO films grown on STO substrates by PLD. AFM images of [010] orientated films showed spontaneous alignment of domains. A *unidirectional* anisotropy was observed; easy axis of magnetization was always perpendicular to the surface of the thin films irrespective of film orientation, which has immense importance in the next generation of magnetic recording media.

ACKNOWLEDGMENTS

The financial support from DEPSCoR under Grants No. W911NF-06-0030 and No. W911NF-05-1-0340 is gratefully acknowledged. R.P. thanks Institute for Functional Nanomaterials (IFN), University of Puerto Rico for financial support.

[1] R. Ramesh and D. G. Schlom, Science **296**, 1975 (2002).
[2] J. F. Scott, Nature Mater. **6**, 256 (2007).
[3] J. F. Scott, Science **315**, 954 (2007).
[4] C. H. Ahn, R. H. Hammond, T. H. Geballe, M. R. Beasley, J. M. Triscone, M. Decroux, Ø. Fisher, L. Antognazza, and K. Char, Appl. Phys. Lett. **70**, 206 (1997).
[5] H. N. Lee, H. M. Christen, M. F. Chisholm, C. M. Rouleau, and D. H. Lowndes, Appl. Phys. Lett. **84**, 4107 (2004).
[6] A. J. Hartmann, M. Neilson, R. N. Lamb, K. Watanabe, and J. F. Scott, Appl. Phys. A: Mater. Sci. Process. **70**, 239 (2000).
[7] L. Klein, J. S. Dodge, T. H. Geballe, A. Kapitulnik, A. F. Marshall, L. Antognazza, and K. Char, Appl. Phys. Lett. **66**, 2427 (1995).
[8] Q. Gan, R. A. Rao, C. B. Eom, J. L. Garrett, and M. Lee, Appl. Phys. Lett. **72**, 978 (1998).
[9] B. S. Kang, J.-S. Lee, L. Stan, L. Civale, R. F. DePaula, P. N. Arendt, and Q. X. Jia, Appl. Phys. Lett. **86**, 072511 (2005).
[10] A. Kanbayasi, J. Phys. Soc. Jpn. **41**, 1876 (1976).
[11] G. Cao, S. McCall, M. Shepard, J. E. Crow, and R. P. Guertin, Phys. Rev. B **56**, 321 (1997).
[12] C. W. Jones, P. D. Battle, P. Lightfoot, and W. T. A. Harrison, Acta Crystallogr., Sect. C: Cryst. Struct. Commun. **45**, 365 (1989).
[13] A. Callaghan, C. W. Moller, and R. Ward, Inorg. Chem. **5**, 1572 (1966).
[14] R. J. Bouchard and J. L. Gillson, Mater. Res. Bull. **7**, 873 (1972).
[15] S. Reich, Y. Tsabba, and G. Cao, J. Magn. Magn. Mater. **202**, 119 (1999).
[16] D. J. Amit, H. Gutfreund, and H. Sompolinsky, Phys. Rev. A **32**, 1007 (1985), and references therein.
[17] K. Binder and A. P. Young, Rev. Mod. Phys. **58**, 801 (1986).
[18] K. H. Fischer and J. A. Hertz, *Spin Glasses* (Cambridge University Press, Cambridge, England, 1993).
[19] *Scanning Probe Microscopy and Spectroscopy: Theory, Techniques, and Applications*, 2nd ed., edited by D. Bonnell (Wiley, New York, 2001).
[20] Scanning Probe Microscopy Software (WSXM), Nanotec. Electronica S. L., 2005.
[21] J. Stöhr and H. C. Siegmann, *Magnetism From Fundamental to Nanoscale Dynamics* (Springer, Berlin, 2006), p. 516.
[22] M. Izumi, K. Nakazawa, Y. Bando, Y. Yonedo, and H. Terauchi, J. Phys. Soc. Jpn. **66**, 3893 (1997).
[23] Q. Gan, R. A. Rao, C. B. Eom, L. Wu, and F. Tsui, J. Appl. Phys. **85**, 5297 (1999).
[24] J. Wang, Nature Mater. **4**, 191 (2005).
[25] M. Vopsaroiu, J. Blackburn, A. Muniz-Piniella, and M. G. Cain, J. Appl. Phys. **103**, 07F506 (2008).
[26] S. Blundell, *Magnetism in Condensed Matter* (Oxford University Press, New York, 2001), p. 119.
[27] L. M. Wang, H. E. Horng, and H. C. Yang, Phys. Rev. B **70**, 014433 (2004).
[28] L. Klein, J. S. Dodge, C. H. Ahn, G. J. Snyder, T. H. Geballe, M. R. Beasley, and A. Kapitulnik, Phys. Rev. Lett. **77**, 2774 (1996).
[29] D. Kim, B. L. Zink, F. Hellman, S. McCall, G. Cao, and J. E. Crow, Phys. Rev. B **67**, 100406(R) (2003).
[30] M. Mueller, U. Köbler, and K. Fisher, Eur. Phys. J. B **8**, 207 (1999).
[31] S. L. Young, H. Z. Chen, L. Horng, J. B. Shi, and Y. C. Chen, Jpn. J. Appl. Phys., Part 1 **40**, 4878 (2001).
[32] S. F. Edwards and P. M. Anderson, J. Phys. F: Met. Phys. **5**, 965 (1975).
[33] M. Gruyters, Phys. Rev. Lett. **95**, 077204 (2005).
[34] S. N. Kaul, Curr. Sci. **88**, 78 (2005).
[35] F. Lefloch, J. Hammann, M. Ocio, and E. Vincent, Physica B **203**, 63 (1994).
[36] X. L. Wang, M. James, J. Horvat, and S. X. Dou, Supercond. Sci. Technol. **15**, 427 (2002).
[37] I. A. Campbell, S. Senoussi, F. Varret, J. Teillet, and A. Hamzić, Phys. Rev. Lett. **50**, 1615 (1983).
[38] S. E. Nagler and B. C. Chakoumakos, Bull. Am. Phys. Soc. **42**, 551 (1997).
[39] I. I. Mazin and D. J. Singh, Phys. Rev. B **56**, 2556 (1997).
[40] A. T. Zayak, X. Huang, J. B. Neaton, and K. M. Rabe, Phys. Rev. B **74**, 094104 (2006).